Non-Hermitian coupled semiconductor laser array

Ramon Herrero [a], Judith Medina Pardell [a], Muriel Botey [a], Kestutis Staliunas [a,b]
[a] Departament de Física, Universitat Politècnica de Catalunya (UPC), Colom 11, E-08222 Terrassa, Barcelona, Catalonia
[b] Institució Catalana de Recerca i Estudis Avançats (ICREA), Passeig Lluís Companys 23, E-08010 Barcelona, Catalonia

We propose and explore a stabilization mechanism of a semiconductor laser array based on asymmetric coupling between neighboring lasers. The stabilization scheme takes advantage of the symmetry breaking of non-Hermitian potentials. We perform a comprehensive numerical analysis in terms of the design parameters, namely the distance between lasers and spatial shift between the individual laser stripe and corresponding electrode. In turn, a mirror-symmetric architecture is intended to lead to a light redistribution within the array which is expected to facilitate direct coupling efficiency to optical fibers.

Keywords: Lasers, Semiconductor lasers, laser array, Non-Hermitian coupling

1. INTRODUCTION

Arrays of Edge-Emitting Lasers (EEL), also known as laser bars or stacks of EEL bars, are replacing other lasers sources due to their compactness, low prices and high performance. However, the spatiotemporal instability and divergence are implicit in this kind of lasers and represent their major drawback for many applications, particularly because it prevents an efficient coupling to optical fibers. While the self-focusing filamentation instabilities and complex dynamical behaviors are typically shown by a single EEL [1,2], the coupling between neighboring EELs in laser bars contributes to increase such spatiotemporal instabilities [3,4]. The consequence is the onset of chaotic and turbulent regimes produced by spatial and temporal instabilities such as the Modulation Instability and Hopf bifurcations.

Some proposals for the regularization of a single semiconductor laser are based on intracavity filtering [5,6] or on the introduction of complex spatial modulations within the laser [7,8,9]. Further, the monomode emission of a single laser is assured by reducing its width, although spatiotemporal instabilities may still arise from the coupling between such monomode lasers in an array. Thus, the stabilization of the EELs bars emission by a compact scheme still is an open question.

We propose a physical stabilization mechanism for arrays of EELs based on the management of the coupling between neighboring lasers. Our proposal is intended to induce a stable emission from the laser array and the improvement of its beam quality. The complex dynamics shown by these laser stacks may be temporally stabilized by the introduction of non-Hermitian potentials combining gain and index profiles with a symmetry breaking. Recently, the interplay between gain and index modulations has emerged in photonics due to its ability of molding the flow of light. The temporal instabilities in EELs may be reduced by simply introducing a lateral shift between a pump profile and an index profile, that is to say a spatial shift between the individual laser stripe and corresponding electrode. In turn the shifts of index profile within the bar are arranged in an axisymmetric architecture, leading to a field concentration at axis, see Figure 1 (a).

We perform a numerical analysis using a complete (2+1)-dimensional space-temporal model, including transverse and longitudinal spatial directions and temporal evolution of the electric field and carriers. We observe regimes of temporal stabilization and light redistribution within the array depending on the design parameters, namely distance between lasers and lateral non-Hermitian shift. The validity of the proposal is also demonstrated for an array with a large number of lasers using a simplified model where the transverse space is accounted by the coupling between the neighboring laser cavities.

2. MODEL OF A SEMICONDUCTOR LASER ARRAY

We use a well-established model that includes the spatiotemporal evolution of the electromagnetic field and carrier density inside the cavity [10]. EELs are class B lasers, for which the material polarization can be disregarded and usually

described either by stationary models [11] or dynamical models of the mean field [12]. To verify the spatial localization and temporal stabilization of the field, a complete spatiotemporal dynamical model is required. It models the spatiotemporal evolution of the carrier density, $N(x,z,t)$, and the forward and backward fields propagating along the 2D space of the laser cavity [13]. The slowly varying envelope approximation is applied for the forward and backward envelopes of the electric field, $A^{\pm}(x,z,t)$, resulting in the following three coupled equations:

$$\pm\frac{\partial A^{\pm}}{\partial z} = \frac{i}{2k_0 n}\frac{\partial^2 A^{\pm}}{\partial x^2} + \sigma[(1-ih)N-(1+\alpha)]A^{\pm} + i\Delta n(x)k_0 A^{\pm} \qquad (1)$$

$$\frac{\partial N}{\partial t} = \gamma(-N-(N-1)\left(\left|A^{+}\right|^2+\left|A^{-}\right|^2\right)^2 + p_0 + \Delta p(x) + D\nabla^2 N)$$

where k_0 is the wavenumber, n is the effective refractive index, σ is inversely proportional to the light matter interaction length, h is the Henry factor of the semiconductor, α corresponds to losses, p_0 is the pump, D is the diffusion of carriers and γ is the relaxation time of the carrier inversion. The wide semiconductor laser is transversally patterned. A stepwise transverse modulations of the refractive index $\Delta n(x)$ accounts for individual laser stripes while the spatial profile of the electrodes, the pump $\Delta p(x\text{-}s)$, follows the same pattern but with a spatial shift s. These two shifted modulations account for the real and imaginary parts of the non-Hermitian potential and lead to an asymmetric coupling between the neighboring lasers, see Fig. 1. (a). Discontinuities in the derivatives of the two spatial transverse profiles are avoided by using sharp sigmoids.

Forward and backward field envelopes can be integrated one after the other in propagation along the EEL cavity assuming constant carriers, because the round-trip time of the cavity is small compared to the carrier's relaxation time. The boundary conditions given by mirrors of the Fabry-Perot cavity are $A^{+}(z=0) = r_0 A^{-}(z=0)$ and $A^{-}(z=L) = r_L A^{+}(z=L)$, where L is the length of the laser and $r_{0/L}$ are the corresponding reflections. The integration of the field in one roundtrip is followed by the temporal integration of carriers considering a constant field.

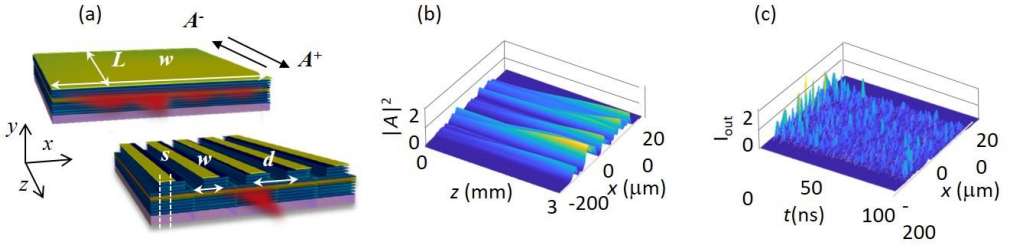

Figure 1. (a) Scheme of a broad single EEL with a laser width w and length L presenting an inhomogeneous and temporally unstable emission, and scheme of the wide semiconductor laser transversally patterned with axial symmetry, i.e. a laser array made of single lasers close one another presenting a lateral shift between pump and index profiles ($s \neq 0$) and separated a small distance d. (b) Intensity of the total field within the wide laser and (c) temporal evolution of the output intensity. Integration parameters: $p_0 = 2.0$, width = 400 μm, $L = 1500$ μm, $\alpha = 0.1$ μm^{-1}, $h = 2.0$, $s = 0.04$ μm^{-1}, $k_0 = 2\pi$ μm^{-1}, $D = 0.03$ cm^2/s, $n = 3$, $r_L = 0.04$ and $r_0 = 0.99$.

3. ASYMMETRIC COUPLING

The stability of the laser array is based on the asymmetric coupling of single lasers. We first analyze the spatiotemporal dynamics of a single EEL and decrease the laser width up to avoid the typical strongly multimode and temporally unstable emission of broad semiconductor lasers. The maximum width for a monomode emission is determined by $w_{max} = \lambda/\sqrt{2n\Delta n}$, corresponds to 4 μm for parameters chosen in Fig.1 and is in good agreement with the numerical integrations of eq. (1).

Once the parameters for a single laser with stable dynamics are determined, we analyze the effect of the coupling between two lasers. Such coupling depends on the distance d between lasers and on the shift s between the laser profile (refractive index profile) and the pump profile. Increasing the symmetric coupling (s=0) between them by reducing their

separation, both lasers become temporally unstable with asymmetric temporal evolutions, see Fig. 2 (a). However, slightly shifting the index profile of both lasers with respect to the gain profiles, we induce an asymmetric coupling, the light generated in one laser is partially transferred to the other and both lasers become temporally stable, see Fig. 2 (b).

We explore the parameter space of the distance between lasers, d, and asymmetry shift parameter, s for a fixed value of the pump. The results are summarized in an enhancement of the intensity of the laser to which the energy is accumulated, relative to the unshifted case, s = 0. This enhancement is visible for small laser distances and balanced shift values, see Fig. 2 (c). In addition, the temporal stability of the emission is evaluated by mapping the amplitude of the temporal oscillations, Fig. 2 (d). Temporal instabilities arise for small d and s values, while stability is found either increasing the coupling asymmetry or, trivially, at large distances between lasers. Interestingly, we observe temporally stable behaviors around the maximum relative intensity region in the parameters space (d, s).

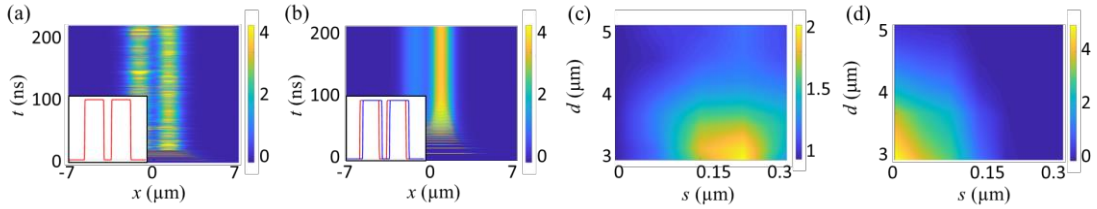

Figure 2. (a)/(b) temporal evolution of the intensity at $z = L$ for two symmetrically/asymmetrically coupled lasers with w = 2.5 μm, separated a center-to-center distance d = 3 μm and for s = 0.25 μm. Insets show the transverse pump profile Δp (red curve) and the index profile Δn (blue curve), and they coincide in (a). (c) Intensity enhancement factor of the amplified laser depending on the distance between lasers, d, and spatial shift, s. (d) Temporal instability map. Relative amplitude of the temporal oscillations. All the integration parameters are the same as in Fig. 1, and p_0 = 2.5.

4. EEL ARRAYS WITH AXISYMMETRIC INWARD COUPLING

Taking advantage of the simultaneous enhancement and temporal stabilization for asymmetric couplings, we propose a simple axisymmetric architecture for EEL arrays. The array is divided into two half-spaces with a symmetric spatial shift between gain and transverse index profiles, arranged such that high index intervals lay closer to the symmetry axis than corresponding gain intervals and the central laser holding no displacement. Such configuration induces an inward coupling directed to axis and it is expected to reach light localization in axis as well as temporally stable regimes given by the asymmetric coupling.

We develop a simplified model to characterize EEL arrays with a large number of lasers. The model accounts for the longitudinal field propagation, temporal evolution and coupling between lasers but disregarding diffraction and carriers diffusion, so disregarding transverse modes of the single laser. The model describes the forward and backward field of every single j laser of the array, namely $A_j^{\pm}$, as monomode lasers in the transverse direction and coupled to the two neighboring lasers, as:

$$\begin{aligned}\frac{\partial A_j^{\pm}}{\partial z} &= \sigma\left[\left(1-ih\right)N-\left(1+\alpha\right)\right]A_j^{\pm}+m^{-}A_{j-1}^{\pm}+m^{+}A_{j+1}^{\pm}\\ \frac{\partial N_j}{\partial t} &= \gamma\left(-N-\left(N-1\right)\left(\left|A^{+}\right|^2+\left|A^{-}\right|^2\right)+p_0\right),\ for\ \ j=-\frac{num-1}{2},\ldots,\frac{num-1}{2}\end{aligned} \tag{2}$$

where, $m^{+/-}$ are complex numbers standing for the coupling parameter from the neighboring lasers at positions j+1 and j-1, respectively, and the spatial and temporal coordinates and all parameters are normalized as in eq. (1). In the simplest case, a periodic non-Hermitic potential in one-dimension may be approximated by a complex harmonic form: $V\left(x\right)=m_m\left[m_r\cos\left(\frac{2\pi}{d}x\right)+im_i\sin\left(\frac{2\pi}{d}x+\Phi\right)\right]=m_m\left[m^{+}e^{+i\frac{2\pi}{d}x}+m^{-}e^{-i\frac{2\pi}{d}x}\right]$, where d is the distance between lasers and m_r and m_i the amplitudes of the real and imaginary part of the non-Hermitian potential. Therefore, from eq. (2) we may express the coupling between neighboring lasers derived from this simple harmonic complex potential as

$m^{\pm} = \left(\frac{m_r \pm m_i}{2}\right)\cos\Phi + im_i \sin\Phi$. The coupling strength m_m has a logarithmic relationship with the laser distance d while the phase shift between the real and imaginary components of the coupling, $\pi/2$-Φ is proportional to the spatial shift s. The model allows to define different types of coupling between two lasers depending on the values of m_r, m_i and the phase, Φ. For $\Phi = \pm \pi/2$, the coupling is perfectly symmetric while for $\Phi = 0$, the coupling becomes Parity-Time (PT) symmetric. For simplicity, we assume the maximally asymmetric coupling, $m_r = m_i = 1$, the PT-symmetry breaking point. The other parameters: σ, h, α, γ and p_0 are the same of eq. (1).

We calculate the spatial redistribution of the generated light, the localization and the light enhancement at the central laser, for axisymmetric arrays of *num* lasers, see Fig. 3. (a). We increase *num* up to 21, a typical laser number for an actual laser bar. We assume $\Phi = 0$, and we scan the number or lasers for strong and weak coupling factors.

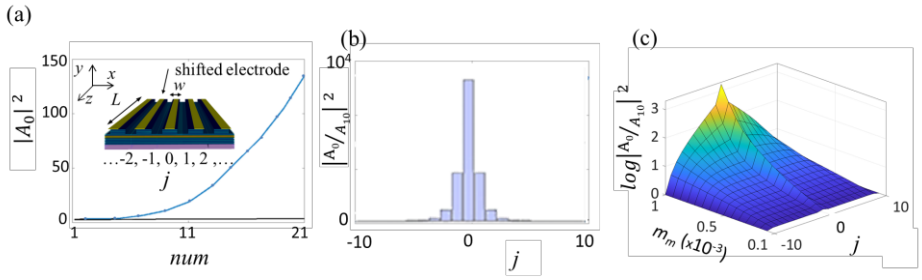

Figure 3. (a) Intensity of the central laser, $|A_0|^2$, for arrays of *num* lasers with inward axisymmetric coupling, for the simplified model, eq. (2), and for two different coupling strengths: $m_m = 10^{-3}$ (blue) and for $m_m = 10^{-5}$ (black). The inset displays the proposed scheme for *num* lasers, j = -(*num*-1)/2…0…(*num*-1)/2, with shifted gain and index profiles. (b) Emitted intensity distribution for an array made of *num* = 21 lasers and $m_m = 2 \cdot 10^{-3}$. Intensity of laser j relative to the laser at edge (j=10) (c) Emitted intensity distribution in logarithmic scale for an 21 laser array as a function of the coupling strength, m_m.

For a given laser array, field localization is clearly visible evaluating the intensity at each laser position (Fig. 3. (b)). Localization can be evaluated as a function of the coupling parameter, see Fig. 3. (c) showing the increase of the energy concentration towards the central laser rapidly increasing with the coupling parameter m_m above a given threshold ($m_m = 10^{-3}$). The peak at the central laser is due to the addition of fields coming from both sides.

For small couplings the output intensity of the central laser remains almost constant increasing the number of lasers but for strong enough couplings the field localization induces a pronounced growth of the output power of the central laser, see Fig. 3. (a). For a weak coupling strength m_m, the gain enhancement in laser j given by the asymmetric coupling from the neighboring laser j+1 (or j-1) is small and the laser losses α limits the field amplitude A_j remaining constant along the array, from the edge lasers to the central laser, with an intensity value about the standing alone laser. In contrast, for large m_m values, the asymmetric coupling strongly enhances gain, and the cascade effect from edges to the central laser is the cause of the energy localization with a sharp profile.

Once we have analyzed laser arrays composed by a large number of lasers with the simplified model, we reproduce the observed behavior with the full model of eq. (1). The smallest axisymmetric configuration, three coupled lasers, is summarized on Fig. 4 (a,b). The three lasers are temporally unstable for the symmetric coupling while introducing an inward asymmetric shift of the index profile versus the gain profile, the generated light tends towards the central laser and all lasers become stable. The evaluation of the parameter space shows a range of maximum energy localization with enhancement ratios about 3 for distances around 3.5 µm, and shift parameter $0.15 \leq s \leq 0.25$. Temporal stability is also achieved for the same range of parameters. The same architecture can support a larger number of lasers obtaining similar behaviors, a larger light localization at axis, enhanced field in the central laser and a stable emission. We have simulated up to 13 lasers array with the full model. The field distribution inside this 13 lasers array with and without non-Hermitian coupling is compared in Fig. 4 (c,d). Note the Gaussian envelope in the transverse profile of Fig. 4 (d) that corresponds to an important increase of the beam quality. Thus, the transverse non-Hermitian coupling presents a twofold benefit, the stabilization of the emission of the laser array as well as an increase of the beam quality.

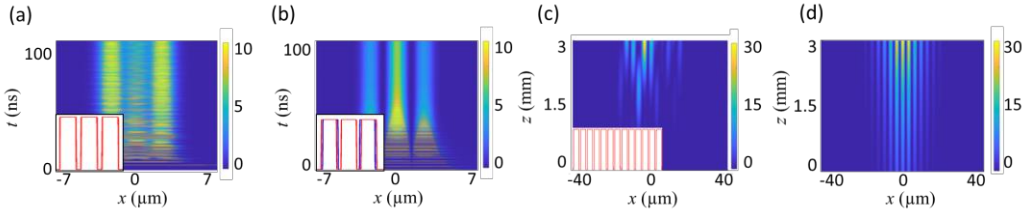

Figure 4. (a)/(b) Temporal evolution of the intensity at $z = L$, proportional to output intensity, for three lasers with symmetric/inward-axisymmetric coupling with w = 2.5 μm, separated a center-to-center distance d = 3.0 μm and for (a) s = 0 (symmetric coupling) and (c) s = 0.25 μm (non-Hermitian coupling). Insets shows the transverse pump profile Δp (red curve) and the index profile Δn (blue curve), and they coincide in (a). Spatial distribution of the intensity inside the laser cavity for a 13 laser array with d = 3.0 μm after sufficient integration time for (c) a symmetric coupling (s = 0) and (d) an axial non-Hermitian coupling (s = 0.25 μm). The rest of integration parameters are the same as in Fig. 1.

Finally, we study the beam quality emitted by non-Hermitian laser arrays by using the full model of eq. (1). The output intensity shows a linear dependence of the output intensity on the number of a lasers and is strongly localized on the central laser allowing a direct coupling to a fiber or to waveguides (Fig. 5 (a)). The beam quality is characterized by the parameter $M^2 = \frac{\pi w \theta}{\lambda}$, where w is the beam waist and θ is the beam divergence, $M^2 = 1$ for the Gaussian beam. The parameter allows us to compare the three cases of Fig. 5. (c): a single broad laser with a width equivalent to the active width of the array (red line), the array with symmetric coupling between lasers (black line) and an axisymmetric inward coupling (blue line). In the first case, M^2 increases exponentially with the width as new modes appear, and the laser becomes highly inhomogeneous. When we introduce the strips, we improve the beam quality, with M^2 increasing linearly with the number of lasers. More interesting is the case of arrays with non-Hermitian inward coupling, which highly increases the beam quality and strongly smooths its dependence on the number of lasers.

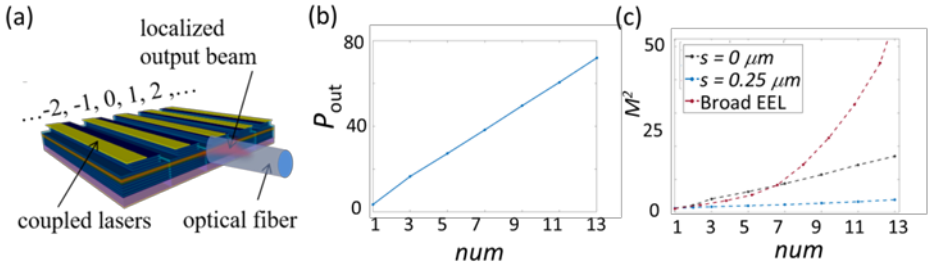

Figure 5. (a) Scheme of the array of coupled lasers directly coupled to an optical fiber. (b) Output power dependence on the number of laser lasers (*num*) for the axisymmetric inward coupling scheme. (c) Dependence of M^2 with the number of lasers (*num*), for three different cases, in red a broad EEL of equivalent width, in black the array of lasers with symmetric coupling, and in blue the array of lasers with axisymmetric inward coupling.

5. CONCLUSIONS

In summary, we propose a physical mechanism for the temporal stabilization and localization of the emission of a coupled array of EELs, an EEL bar.

The scheme is based on a non-Hermitian coupling between neighboring lasers with an axisymmetric geometry. While the monomode emission of a single laser is assured by reducing its width, spatiotemporal instabilities may still arise from the coupling between lasers in the array. Such temporal instabilities are molded by a non-Hermitian coupling that may be

simply introduced by a lateral shift between the pump and index profile, technically by a spatial shift between the individual laser stripe and corresponding electrode. Such asymmetric coupling, while temporally stabilizing the emission also redistributes and localizes energy close to the central symmetry axis.

The proposed stabilization scheme is analyzed by a complete spatiotemporal model, including transverse and longitudinal spatial directions and the temporal evolution of the electric fields and carriers. We perform a numerical analysis in parameters space, like the distance between lasers and shift between pump and refractive index, observing regimes of simultaneous temporal stabilizations and light localization. The proposal validity is also demonstrated for an array with a large number of lasers using a simplified model where the transverse space is accounted by the coupling between neighboring laser cavities.

The proposed non-Hermitian architecture for stable EEL bars leads to a bright and temporally stable output beam. The axial concentration of the field is expected to facilitate a direct coupling of these semiconductor lasers arrays to an optical fiber or a waveguide, eventually avoiding any optical elements and minimizing losses.

REFERENCES

[1] O. Hess, S. W. Koch, and J. V. Moloney, "Filamentation and beam propagation in broad-area semiconductor lasers," IEEE J. Quantum Electron. **31**, 35 (1995).

[2] H. Adachihara, O. Hess, E. Abraham, and J. V. Moloney, "Spatiotemporal chaos in broad-area semiconductor lasers,**"** J. Opt. Soc. Am. B **10**, 496 (1993).

[3] S. Yanchuk, A. Stefanski, T. Kapitaniak, and J. Wojewoda, "Dynamics of an array of mutually coupled semiconductor lasers," Phys. Rev. E **73**, 016209 (2006).

[4] H. G. Winful, and L. Rahman, "Synchronized chaos and spatiotemporal chaos in arrays of coupled lasers," Phys. Rev. Lett. **65**(13), 1575-1577 (1990).

[5] D. Gailevicius, V. Koliadenko, V. Purlys, M. Peckus, V. Taranenko, and K. Staliunas, "Photonic crystal microchip laser," Sci. Rep. 6(1), 1-5 (2016).

[6] S. Gawali, J. Medina, D. Gailevičius, V. Purlys, G. Garre-Werner, C. Cojocaru, J. Trull, M. Botey, R. Herrero, J. Montiel-Ponsoda, and K. Staliunas, "Spatial filtering in edge-emitting lasers by intracavity chirped photonic crystals," JOSA B 37(10), 2856-2864 (2020).

[7] R. Herrero, M.Botey, M. Radziunas, and K. Staliunas, "Beam shaping in spatially modulated broad-area semiconductor amplifiers," Opt. Lett. 37(24), 5253-5255 (2012).

[8] S. Kumar, R. Herrero, M. Botey, and K. Staliunas, "Suppression of modulation instability in broad area semiconductor amplifiers," Opt. Lett. 39(19), 5598-5601 (2014).

[9] W. W. Ahmed, J. Medina, R. Herrero, M. Botey, and K. Staliunas, "Stabilization of Broad-area semiconductor laser sources by simultaneous index and pump modulations," Opt. Lett. 43(11), 2511-2514 (2018).

[10] W. W. Ahmed, J. Medina, R. Herrero, M. Botey, and K. Staliunas, "Stabilization of Broad-area semiconductor laser sources by simultaneous index and pump modulations," Opt. Lett. 43(11), 2511-2514 (2018).

[11] G. P. Agrawal, "Fast-Fourier-transform based beam-propagation model for stripe-geometry semiconductor lasers: Inclusion of axial effects," J. Appl. Phys. 56, 3100 (1984).

[12] E. A. Ultanir, D. Michaelis, F. Lederer, and G. I. Stegeman, "Stable spatial solitons in semiconductor optical amplifiers," Opt. Lett. 28(4), 251-253 (2003).

[13] J.M. Pardell, R.Herrero, M.Botey and K.Staliunas, "Non-Hermitian arrangement for stable semiconductor laser arrays", Optics express, 29(15), 23997-24009 (2021).